Int. J. Appl. Comput. Math (2022) 8:239
https://doi.org/10.1007/s40819-022-01446-7

ORIGINAL PAPER

Impressions of Casson $CuO - TiO_2/EG$ Non-Darcian Viscous Dissipative Flow Casson Hybrid Nanofluid Non-Darcian Flow

N. Indumathi[1] · B. Ganga[2] · S. Charles[3] · P. Renuka[4] · A. K. Abdul Hakeem[1]

Accepted: 2 August 2022 / Published online: 29 August 2022

Abstract
The movement and heat transmission of viscous dissipative Casson hybrid nanoliquid (cupric oxide CuO– titania TiO_2/ethylene glycol EG) flow across a flat sheet saturated with non-Darcy porous medium and forced convection were the focus of this investigation. The major partial differential equalities besides the limit conditions were condensed to dimensionless forms by using proper similarity transformation. The follow-on system of ODEs by the matching limit conditions was elucidated numerically by way of MATLAB and the bvp4c solver. The research results are investigated for simple TiO_2/EG and hybrid $CuO - TiO_2/EG$ nanoliquids. As far as important reactions are concerned, the larger Casson parameters upsurge the velocity and decline the temperature profile. Over and above that, porosity and Eckert number are strengthened by the thermal field. However, the Nusselt number increases for the enhancement of the porous resistance parameter and decreases for the enhancement of the Eckert number and porosity parameter. Also, comparison with the available one is also rendered as a special case of our analysis.

Keywords Viscous dissipation · $CuO - TiO_2 - EG$ · non-Darcy porous medium · Hybrid nanofluid

Mathematics Subject Classification 76DXX

Introduction

Nanoliquid is a colloidal suspension with nanoparticles distributed evenly in the base liquid and has many special characteristics in the field of engineering technology. For last two decades, exploratory study of the structure and the thermal transfer properties of nanoliquids has developed drastically due its large usage in many research and manufacturing

✉ A. K. Abdul Hakeem
abdulhakeem6@gmail.com

[1] Department of Mathematics, Sri Ramakrishna Engineering College, Coimbatore 641 022, India

[2] Department of Mathematics, Providence College For Women, Coonoor 643 104, India

[3] Department of Mathematics, PSG College of Arts and Science, Coimbatore 641014, India

[4] Department of Mathematics, KPR Institute of Engineering and Technology, Coimbatore 641 407, India

applications like energy storage, inorganic chemicals, heating and ventilation processes and microelectronics. The cooling properties of an ethylene glycol (EG)-based nanofluid including three nanomaterials aluminium oxide (Al_2O_3), titanium dioxide (TiO_2) and copper oxide (CuO) are investigated by Mutuku [1]. She finalized that, at the boundary layer, $CuO - EG$ nanofluid causes a rapid drop in temperature compared with $TiO_2 - EG$ and $Al_2O_3 - EG$. Kumaresan et al. [2] found that the copper oxide nanofluid has a lower velocity than the magnesium oxide nanofluid when compared with the heat transfer effects of CuO/H_2O and MgO/H_2O across a porous embedded stretched sheet. Rana et al.[3] found that the nanoliquid (TiO_2/EG) heat transfer and its boundaries are accelerated by the quadratic thermal radiative heat flux. Shaiq et al. [4] enquired the thermophysical characteristics and form factor of two nanofluids, $TiO_2 - EG$ and $Cu - EG$, and found that skin friction is higher for copper nanoparticles and lower in the presence of titanium dioxide. The market for compact electronic components and devices have increased rapidly, demanding more efficient thermal conductivity related to the nanoliquid, hybrid nanoliquid is deliberated to be a fresh form of nanoliquid and is more required to develop the ability for transmission of heat. In general, dual strategies are meant for the production of hybrid nanoliquids are either produced by dissipating various forms of nanoparticles in the base liquid or by dissipating the hybrid form of nanoparticles in the base liquid.

Various analytical, theoretical, experimental and numerical research has been carried out by investigators on hybrid nanoliquid heat transfer. Aladdin and Bachok [5] examined on $Al_2O_3 - TiO_2/water$ and finalized that hybrid nanoliquid escalates skin friction and decelerates Nusselt number. Sadaf and Abdesalam [6] proposed a model based on a hybrid nanofluid containing nanoparticles ($Ag + Al_2O_3$) that will be effective for applications connected to metabolic structures that play a critical role in heat sources inside the human body. According to Khashi'ie et al. [7], the establishment of the Eckert number has no effect on the boundary layer split–up, but it does reduce the heat transfer rate of $Cu - Al_2O_3/H_2O$ flow over a stretching/shrinking plate. When compared to nanofluid, the hemodynamic velocity of hybrid nanofluid is higher, according to Abdelsalam et al. [8]. The Marangoni convective boundary on hybrid nanoliquid was explored by Aly and Ebaid [9], and it was discovered that as the nanoliquid expanded in the porous holes, the velocity and heat distribution increased and decreased, respectively. Hayat et al. [10] discovered that the required amount of heat transfer can be achieved by using distinct and appropriate nanoparticle scopes in hybrid nanoliquid. Eshgarf et al. [11] reviewed the models, preparation, stability, and properties of hybrid nanoliquid forthrightly.

Non-Newtonian viscosity properties are primarily used in the biochemical engineering world. Non-Newtonian fluids do not obey the law of viscosity; any classified liquid can achieve density increases of two or three orders of magnitude, which are not negligible in the polymer phase. As a result, Isaac Newton's concept of non-Newtonian dynamics gained popularity. Abdelsalam et al. [12] examined the electromagnetic flow of the Eyring–Powell fluid model for transient flow in non–Newtonian fluid. Raza et al. [13] developed the Williamson fluid model for non–Newtonian fluids as an application of solar energy in thermal engineering operations. Adewale et al. [14] tested the models for non-Newtonian liquids and discovered that the Casson physiochemical model accurately characterised in both low and high tensile environments. Aman et al. [15] studied the Casson hybrid $Cu - Al_2O_3$/Sodium Alginate with Caputo time fractional derivative and concluded that the volume fraction declines the velocity and elucidates the temperature field. Jamshed and Aziz [16] investigated the different shapes of nano particles and concluded that lamina–shaped particles have the highest temperature for $CuO - TiO_2/EG$ Casson model flow past a stretching sheet.

Heat exchange in porous media does have an extensive variety of applications. Different industrial implementations have been experienced, where a certain porous medium is established. There are signal recognition cooling systems, temperature control, tidal energy fields, oil production, nuclear waste disposal components, and so on. The Darcy movement was exemplified, as evidenced by references [17–23]. Plentiful issues with non–Darcy movement situations in porous media of either Newtonian or non–Newtonian liquid have been deliberated in [24–29].

Viscous dissipation is really a minor consequence and its impact can become significant when the viscosity of the liquid is quite large. This alters thermal performance by having a part as a source of power. That contributes to something like the heat flux being influenced. It is understood by Anuar et al. [30] that viscous hybrid nanoliquid has an additional chilling effect than nanoliquid. Elmabouda et al. [31] studied the peristaltic motion of an incompressible fluid with varying viscosity generated by a periodic sinusoidal travelling wave along the tube walls. Sreenivasulu et al. [32] concluded that the temperature difference from the liquid to the surface is low while the Eckert number is lower in each of the $x - y$ directions.

Owing to its broad and extensive uses in engineering and manufacturing processes, plastic extrusion, fibre and cable undercoat, food packaging, paper processing and liquid fuels flow past flat surfaces, attracting a great deal of interest. This investigation focuses on the numerical study of non–Newtonian $CuO - TiO_2/EG$ hybrid nanoliquid, non–Darcy, viscous dissipative flow past a flat sheet with forced convection.

Mathematical Formulation

Figure 1 explains a steady, two dimensional (x, y), forced convective, viscous type Casson hybrid nanoliquid flow over a flat plate through a non–Darcy porous medium. The base liquid (Ethylene Glycol) is in thermal balance with the nanoparticles (cupric oxide CuO and Titania TiO_2) and there is no contact between the two solid components. Table 1 shows CuO, TiO_2 and EG (nanoparticles and base liquid) thermophysical properties. The flat sheet is on the x-axis and the y-axis is taken in a direction perpendicular to the sheet. u_∞ velocity is found on the free surface. The research involves the formulation of boundary layers. We account for the fact that frictional heating due to viscous dissipation as the liquid considered in this

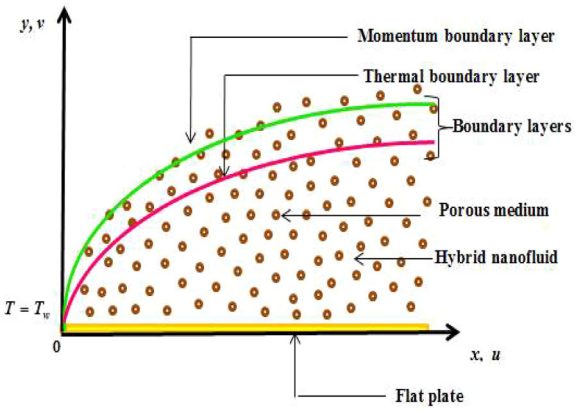

Fig. 1 Physical Configuration

Table 1 Thermophysical properties of nanoparticles and base liquid Jamshed and Aziz [19] Khan et al. [35]

Properties	$\rho(kg/m^2)$	$C_p(J/kgK)$	$K(W/mK)$	$\sigma(S/m)$	Pr
CuO	6510	540	18	5.96×10^7	
TiO_2	4250	686.2	8.9538	2.38×10^6	
EG	1114	2415	0.252	5.5×10^{-6}	204

study is of a non–Newtonian form. The plate is impermeable. The dissipation of Joule is known to be insignificant.

The rheological state equation of the hybrid nanoliquid form of Casson is expressed as(Ahmad and Nadeem [33])

$$\tau_{cd} = \begin{cases} 2\left(\mu_P^* + \frac{S_y^*}{\sqrt{2\pi}}\right) e_{cd}, \pi > \pi_c^* \\ 2\left(\mu_P^* + \frac{S_y^*}{\sqrt{2\pi_c^*}}\right) e_{cd}, \pi < \pi_c^* \end{cases} \tag{1}$$

Where $\pi = e_{cd}e_{cd}$ is $(c, d)^{th}$ components of deformation and π_c^* is called the critical value, S_y^* is the yield stress and μ_P^* is the plastic viscosity. So, the set of governing equations of the hybrid nanoliquid movement is [19, 20, 34],

$$u_x + v_y = 0 \tag{2}$$

$$uu_x + vu_y = \nu_{hnl}\epsilon\left(1 + \frac{1}{\beta}\right)u_{yy} - \nu_{hnl}\frac{\epsilon^2}{K}\left(1 + \frac{1}{\beta}\right)u - Fu^2 \tag{3}$$

$$uT_x + vT_y = \alpha_{hnl}T_{yy} + \frac{\mu_{hnl}}{(\rho C_P)_{hnl}}\left(1 + \frac{1}{\beta}\right)u_{yy} \tag{4}$$

with forced convective, uniform free stream, impermeable, isothermal and no slip boundary condition

$$\begin{aligned} &u = v = 0, \quad T = T_w \ \text{ at } \ y = 0 \\ &u \to u_\infty, \quad T \to T_\infty \ \text{ as } \ y \to \infty \end{aligned} \tag{5}$$

where u and v are the velocity components along x and y axis respectively, β is the Casson liquid parameter, ν, ρ, α, μ and C_P are kinematic viscosity, density, thermal diffusivity, dynamic viscosity and specific heat respectively. The thermophysical properties of hybrid nanoliquid are tabulated in Table 2. The subscript hnl denotes hybrid nanoliquid($TiO_2 - CuO/EG$). The subscripts x and y denotes the partial differentiation with respect to x and y respectively. $K, \epsilon, F = C_b\epsilon^2/\sqrt{K}$ are permeability, porosity and Forchheimer coefficient of porous media respectively. Whereas, C_b is the drag coefficient.

Then, we are implementing the following transformations of similarity (Qawasmeh et al.[36])

$$\begin{aligned} &\psi(x, y) = (\nu_f u_\infty x)^{1/2} f(\eta), \ \eta = \frac{y}{x}(Re_x)^{1/2} \ \text{ where } \ Re_x = \frac{u_\infty x}{\nu_f} \\ &u = \frac{\partial \psi}{\partial y}, \quad v = -\frac{\partial \psi}{\partial x} \\ &u = u_\infty f'(\eta), \ v = \frac{-u_\infty}{2} Re_x^{-1/2}(f(\eta) - \eta f'(\eta)) \\ &T = T_\infty + (T_w - T_\infty)\theta(\eta) \end{aligned} \tag{6}$$

Table 2 Thermophysical properties of hybrid nanoliquid

Properties	Hybrid nanoliquid
μ_{hnl}	$\frac{\mu_1}{(1-\phi_1)^{2.5}(1-\phi_2)^{2.5}}$
ρ_{hnl}	$\{(1-\phi_2)[(1-\phi_1)]\rho_l + \phi_1\rho_{s_1}]\} + \phi_2\rho_{s_2}$
ρC_{hnl}	$\{(1-\phi_2)[(1-\phi_1)]\rho C_l + \phi_1\rho C_{s_1}]\} + \phi_2\rho C_{s_2}$
α_{hnl}	$\frac{k_{hnl}}{(\rho C_p)_{hnl}}$
$\frac{\sigma_{hnl}}{\sigma_{nl}}$	$\frac{\sigma_{s_2}+2\sigma_{nl}-2\phi_2(\sigma_{nl}-\sigma_{s_2})}{\sigma_{s_2}+2\sigma_{nl}+\phi_2(\sigma_{nl}-\sigma_{s_2})}$
	Where $\frac{\sigma_{nl}}{\sigma_l} = \frac{\sigma_{s_1}+2\sigma_l-2\phi_1(\sigma_l-\sigma_{s_1})}{\sigma_{s_1}+2\sigma_l+\phi_1(\sigma_l-\sigma_{s_1})}$
$\frac{k_{hnl}}{k_{nl}}$	$\frac{k_{s_2}+(n-1)k_{nl}-(n-1)\phi_2(k_{nl}-k_{s_2})}{k_{s_2}+(n-1)k_{nl}+\phi_2(k_{nl}-k_{s_2})}$
	Where $\frac{k_{nl}}{k_l} = \frac{k_{s_1}+(n-1)k_l-(n-1)\phi_1(k_l-k_{s_1})}{k_{s_1}+(n-1)k_l+\phi_1(k_l-k_{s_1})}$

Using Eq. (6) and table 2, Eqs. (2) to (5) becomes

$$C_1\epsilon\left(1+\frac{1}{\beta}\right)f'''(\eta) + \frac{1}{2}f(\eta)f''(\eta) - \epsilon^2 C_1\alpha(x)\left(1+\frac{1}{\beta}\right)f'(\eta) - \gamma(x)f'(\eta)^2 = 0 \quad (7)$$

$$C_2\theta''(\eta) + C_3 Prf(\eta)\theta'(\eta) + C_4 EcPr\left(1+\frac{1}{\beta}\right)f''(\eta)^2 = 0 \quad (8)$$

with boundary conditions

$$\begin{aligned} &f'(0),\ f(0) = 0,\ \theta(0) = 1 \text{ at } \eta = 0 \\ &f'(\eta) \to 1,\ \theta(\eta) \to 0 \text{ as } \eta \to \infty \end{aligned} \quad (9)$$

For which superscripts denote differentiation with respect to η.
Where

$$C_1 = 1/\left[\left((1-\phi_1)^{2.5}(1-\phi_2)^{2.5}\right)\left((1-\phi_1) + (\phi_1\rho_{s_1}/\rho_l) + (\phi_2\rho_{s_2}/\rho_l)\right)\right],$$

$$C_2 = k_{nl}k_{hnl},$$

$$C_3 = \left((1-\phi_2)((1-\phi_1) + (\phi_1\rho_{s_1}C_{p_{s_1}})/(\rho_l C_{p_l}))\right) + (\phi_2\rho_{s_2}C_{p_{s_2}})/(\rho_l C_{p_f}),$$

$$C_4 = 1/\left((1-\phi_1)^{2.5}(1-\phi_2)^{2.5}\right).$$

Here $\alpha(x) = \nu_l x/u_\infty K$ is the first order porous resistance parameter, $\gamma(x) = Fx$ is the second order porous resistance parameter, $Pr = \mu_l C_{P_l}/k_l$ is the Prandtl number, $Ec = u_\infty^2/C_{P_l}(T_w - T_\infty)$ is the Eckert number.

Physical quantities skin friction coefficient C_f and local Nusselt number Nu, Which have now been described as

$$C_f = \frac{\tau_w}{\rho_l u_\infty^2}, \text{ where } \tau_w = \mu_{hnl}\left(1+\frac{1}{\beta}\right)u_y\big|_{y=0} \quad (10)$$

$$Nu = \frac{xq_w}{k_l(T_w - T_\infty)}, \text{ where } q_w = -k_{hnl}T_y\big|_{y=0} \quad (11)$$

Using transformation of similarity Eqs. (6), (10) and (11) becomes

$$Re_x^{1/2} C_f = \left(1 + \frac{1}{\beta}\right) \frac{f''(0)}{(1-\phi_1)^{2.5}(1-\phi_2)^{2.5}} \tag{12}$$

$$Re^{-1/2} Nu = \frac{-k_{hnl}}{k_l} \theta'(0) \tag{13}$$

Numerical Simulation Methodology

The bvp4c feature of MATLAB is used to achieve the numerical results for cupric oxide–Titania/ethylene glycol. Research results are graphically presented with an emphasis on mathematical key aspects of the model and their effect on velocity, temperature and engineering interest quantities. The first ever step is to list the $3^r d$ order ODEs (7) to (9) as a first-order scheme of ODEs.

$$\begin{aligned}
f &= \Lambda(1) \\
f' &= \Lambda(2) \\
f'' &= \Lambda(3) \\
f''' &= \Lambda(3)' \\
&= -(C_1\epsilon(1+\beta^{-1}))^{-1} \left\{\tfrac{1}{2}\Lambda(1)\Lambda(3) + \epsilon^2 C_1 \alpha(1+\beta^{-1})\Lambda(2) - \gamma\Lambda(2)^2\right\} \\
\theta' &= \Lambda(5) \\
\theta'' &= \Lambda(6) = -Pr{C_2}^{-1} \left\{C_3\Lambda(1)\Lambda(5) + C_4 Ec(1+\beta^{-1})\Lambda(3)^2\right\}
\end{aligned} \tag{14}$$

with limiting equations

$$\begin{aligned}
&\Lambda_0(1) = 0, \quad \Lambda_0(2) = 0, \quad \Lambda_0(4) = 1 \\
&\Lambda_\infty(2) = 1, \quad \Lambda_\infty(4) = 0,
\end{aligned} \tag{15}$$

Equations (14) and (15) are numerically covered as well as the initial value problem to the terminal point. All of these simplifications are done by using the bvp4c feature available in the MATLAB programme.

Results and Discussion

The accuracy of the above–mentioned numerical analysis is accepted by positive correlations with previous reports in a set of cases listed in table 3. It is stated that the current findings are in strong agreement with the reported findings. Each of the Figs.2–12 was designed using the parameters $\phi_1 = \phi_2 = 0.09$, $\epsilon = 0.5$, $\beta = 0.5$, $\alpha(x) = 0.02$, $\gamma(x) = 0.01$, $Pr = 204$, and $Ec = 0.01$.

An upsurge in porosity ϵ reduces velocity in Fig. 2 solution for hybrid nanoliquid ($\phi_1 = \phi_2 = 0.09$) and nanoliquid ($\phi_1 = 0, \phi_2 = 0.09$). Likewise, upward ϵ broadens the flow field boundary layer width. Such a pattern is due to the impact of relatively high porous persistence and thus low permeability. It is shown that these profiles comply asymptotically with the far–field boundary condition, $f'(\infty) = 1$, which confirms the obtained numerical results.

Figure 3 portrays the improvement of velocity for various Casson parameter β for hybrid nanoliquid and nanoliquid. Physically, raising the yield stress of raising the value of β improves the fluid viscosity for both $TiO_2 - CuO/EG$ hybrid nanoliquid and TiO_2/EG

Table 3 Amount of $-\theta'(0)$ for certain Prandtl number with $\varepsilon = 1, \alpha(x) = 0, \gamma(x) = 0$ for Newtonian liquid when $\beta \to \infty$

Pr	Current Study	Qawasmeh et al. [36]	Chamkha et al. [37]	Lin and Lin [38]
10^0	0.33209859	0.332054	0.332173	0.332058
10^1	0.72827071	0.728136	0.72831	0.728148
10^2	1.57190700	1.571821	1.57218	1.57186
10^3	3.38734448	3.387073	3.38809	3.38710
10^4	7.29840868	7.297260	7.30080	7.29742

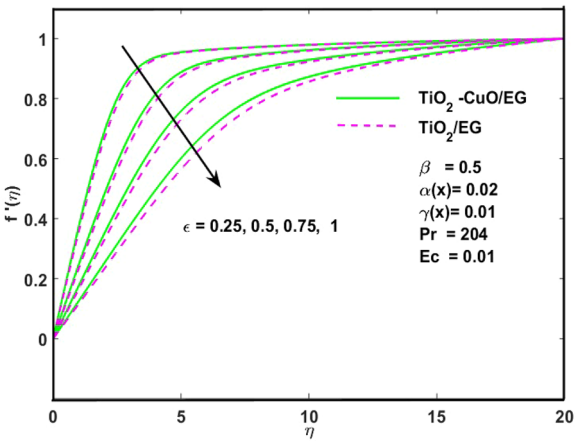

Fig. 2 Influence of porosity ε on velocity profile

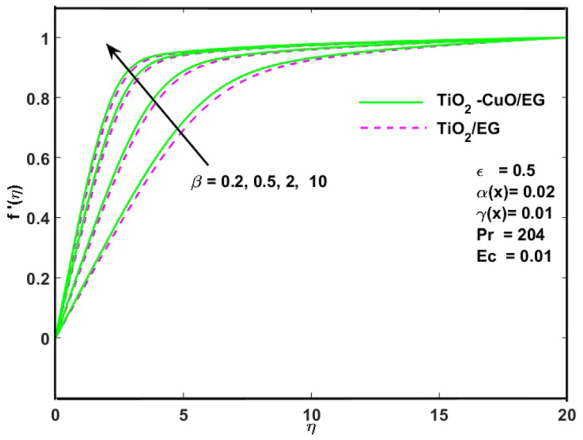

Fig. 3 Influence of Casson parameter β on velocity profile

nanoliquid, which is accountable for the provided variation in fluid momentum. While β hits the infinity challenge in the specific scenario, it is simplified to the Newtonian case.

The rise of the first order porous barrier drags $\alpha(x)$ results in a lower velocity. This can be seen in Fig. 4 and is linked to the improvement of the solid phase's mixed compressive stresses and the solid phase's beneficial expansion. In addition, an increase in the $\alpha(x)$ shortens the velocity boundary layer thickness for hybrid nanoliquids. It is traced back to the additional

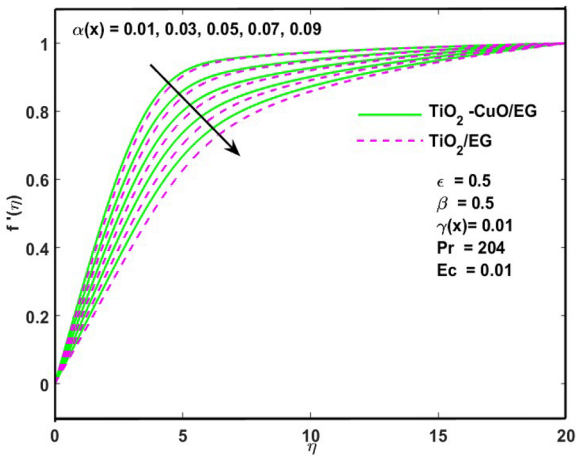

Fig. 4 Influence of first order porous resistance parameter $\alpha(x)$ on velocity profile

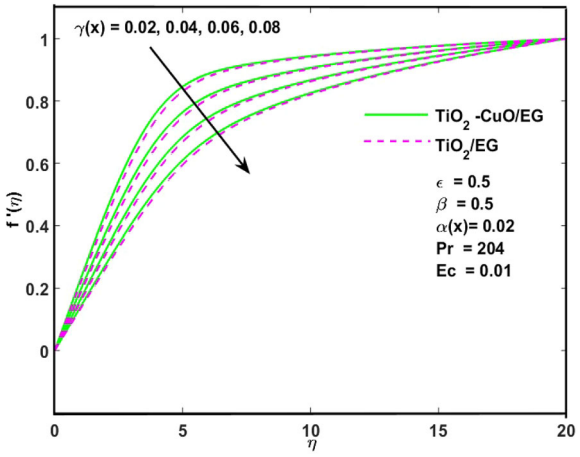

Fig. 5 Influence of second order porous resistance parameter $\gamma(x)$ on velocity profile

compressive stress between the liquid layers due to the combination of the Casson liquid as opposed to the forces acting on that same solid phase.

Figure 5 depicts the effects of second-order porous barrier drag $\gamma(x)$ on the boundary layer velocity field for $CuO - TiO_2/EG$ and TiO_2/EG. We notice that the flow value now lowers as $\gamma(x)$ improves. It highlights the impact of the use of non–Newtonian Casson liquid along with the use of Forchheimer's quadratic drift porous material.

The augmentation in porosity ϵ would raise the temperature is displayed in Fig. 6. In addition, increasing porosity enlarges the boundary layer thickness heat for hybrid nanoliquid and nanoliquid. The entire phenomenon is owing to a high degree of relatively high porous friction and thus low solubility.

Figure 7 shows that the temperature curves drop with just a change in the Casson parameter β. Escalating β, i.e. compression strength minimizes the velocity of the liquid. The temperature curves demonstrate in Fig. 7 that the proportion of travel is substantially reduced by an upsurge of β.

Observing the plots in Fig. 8 indicates that the influence of Eckert number Ec intensifying values is to surge the temperature distribution in the movement area. This is because that

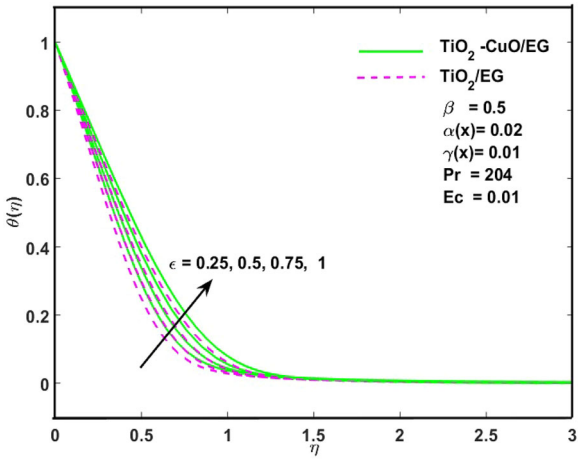

Fig. 6 Influence of porosity ε on temperature profile

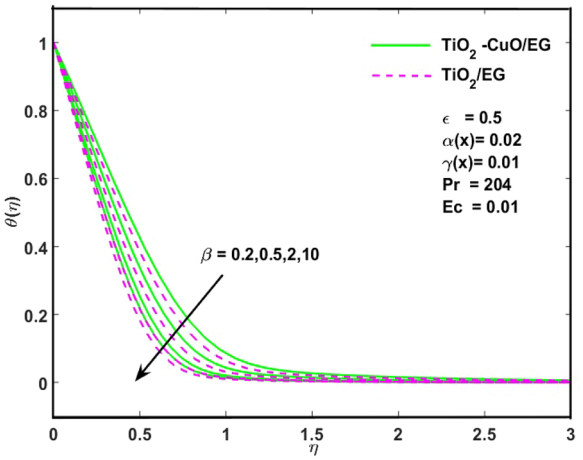

Fig. 7 Influence of Casson parameter β on temperature profile

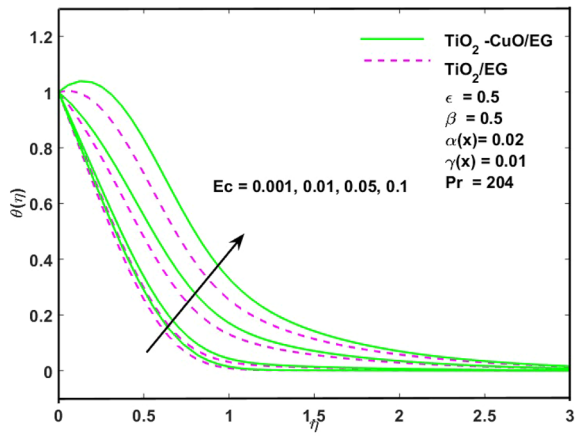

Fig. 8 Influence of Eckert number Ec on temperature profile

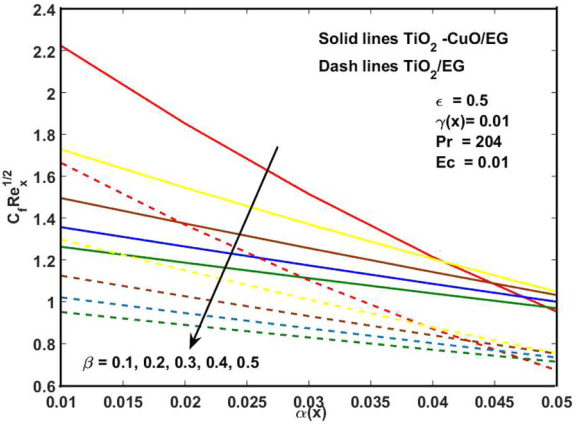

Fig. 9 Illustration of skin friction for certain Casson parameter β and first order porous resistance parameter $\alpha(x)$

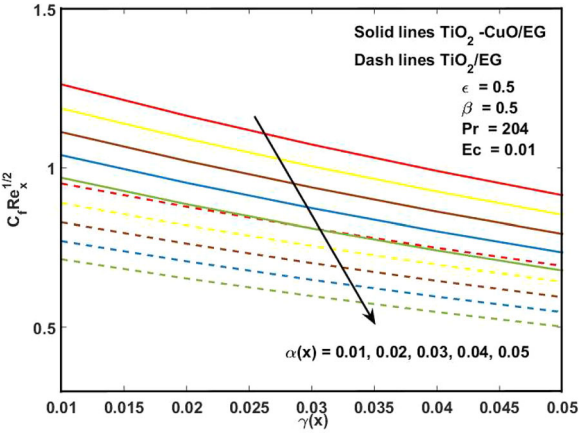

Fig. 10 Illustration of skin friction for certain second order porous resistance parameter $\gamma(x)$ and first order porous resistance parameter $\alpha(x)$

heat energy is contained in the liquid as a result of frictional heating. The effect of growing Ec is to accelerate the temperature of hybrid nanoliquid and nanoliquid.

Figure 9 plots the skin friction for various values of the Casson parameter β and first order porous barrier drag $\alpha(x)$. The escalating scale of β and $\alpha(x)$ declines skin friction. The influence of $\alpha(x)$ and second-order porous barrier drag $\gamma(x)$ on skin friction coefficient is shown in Fig. 10. As a result, the skin friction decreases for $\alpha(x)$ and $\gamma(x)$.

Figure 11 exhibits the Nusselt number for different Ecert number Ec and porosity ϵ. The results show that increasing Ec decreases epsilon and increases Nusselt number. The influence of various Ec and $\alpha(x)$ on Nusselt number illustrated in Fig. 12. For a greater quantity of Ec and $\alpha(x)$ the Nusselt number falls and boosts respectively.

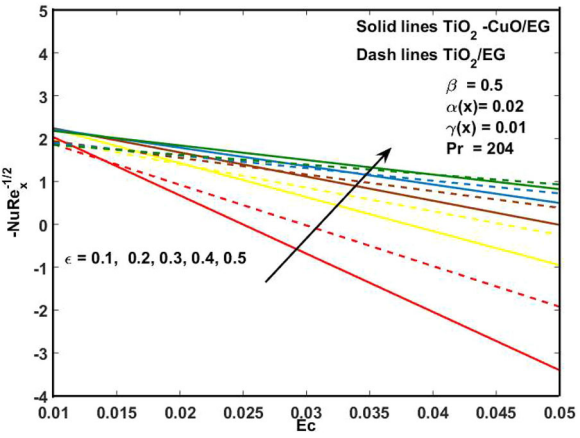

Fig. 11 Illustration of Nusselt number for certain Eckert number Ec and porosity ε

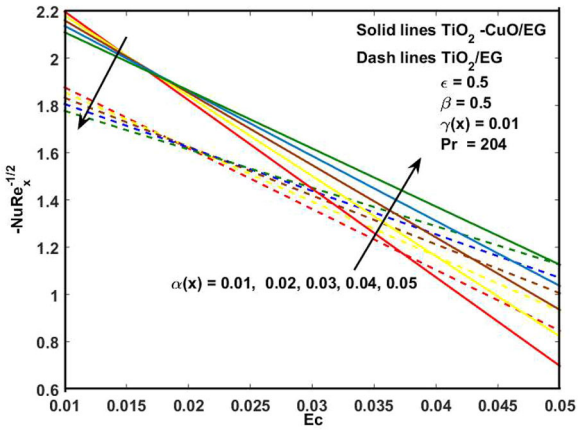

Fig. 12 Illustration of Nusselt number for certain Eckert number Ec and first order porous resistance parameter $\alpha(x)$

Conclusion

The current study looks at numerical learning in a viscous dissipative boundary layer flow all over a porous flat plate with a forced convective limiting condition for hybrid nanoliquid $(CuO - TiO_2/EG)$ and nanoliquid (TiO_2/EG). Numerically, bvp4c in the MATLAB feature was engaged to elucidate the problem. Following results, behaviour was common for both hybrid nanoliquid $(CuO - TiO_2/EG)$ and nanoliquid (TiO_2/EG)

- The completed exploration revealed that the porosity decelerates the velocity and accelerates the temperature distribution and Nusselt number.
- The hiking value of the Casson parameter improves the velocity profile and declines the temperature profile with skin friction.
- The first order and second order porous barriers drag in increment, lowering the velocity field and skin friction. In particular, the first order porous barrier drag increases the heat transfer rate.
- Finally, the enhancing value of the Eckert number strengthens the thermal distribution and weakens the Nusselt number.

Funding The authors have not disclosed any funding.

Data Availability Enquiries about data availability should be directed to the authors.

Declarations

Competing Interests The authors have not disclosed any competing interests.

References

1. Mutuku, W.N.: Ethylene glycol (EG)-based nanofluids as a coolant for automotive radiator. Asia Pac. J. Comput. Engin. **3**(1), 1–15 (2016)
2. Kumaresan, E., Vijaya Kumar, A.G., Rushi Kumar, B.: Chemically reacting on MHD boundary layer flow of $CuO-$water and $MgO-$water nanofluids past a stretching sheet in porous media with radiation absorption and heat generation/absorption. IOP Conf. Series: Materials Sci. Eng. **263**, 062017 (2017)
3. Rana, P., Al-Kouz, W., Mahenthesh, B., Mackolil, J.: Heat transfer of $TiO_2 - EG$ nanoliquid with active and passive control of nanoparticles subject to nonlinear Boussinesq approximation. Int. Commun. Heat Mass Transf. **126**, 105443 (2021)
4. Shaiq, S., Maraj, E.N., Iqbal, Z.: A comparative analysis of shape factor and thermophysical properties of electrically conducting nanofluids $TiO_2 - EG$ and $Cu - EG$ towards stretching cylinder. Chaos, Solitons Fractals **118**, 290–299 (2019)
5. Aladdin, N.A.L., Bachok, N.: Boundary Layer Flow and Heat Transfer of $Al_2O_3 - TiO_2$/Water Hybrid Nanofluid over a Permeable Moving Plate. Symmetry. **12**, 1064 (2020)
6. Sadaf, H., Abdelsalam, S.I.: Adverse effects of a hybrid nanofluid in a wavy non-uniform annulus with convective boundary conditions. RSC Adv. **10**(26), 15035–15043 (2020). https://doi.org/10.1039/D0RA01134G
7. Khashi'ie, N.S., Md Arifin, N., Nazar, R., Hafidzuddin, E.H., Wahi, N., Pop, I.: Magnetohydrodynamics (MHD) axisymmetric flow and heat transfer of a hybrid nanofluid past a radially permeable stretching/shrinking sheet with Joule heating. Chin. J. Phys. **64**, 251–263 (2019)
8. Abdelsalam, S.I., Mekheimer, K.S., Zaher, A.Z.: Alterations in blood stream by electroosmotic forces of hybrid nanofluid through diseased artery: Aneurysmal/stenosed segment. Chin. J. Phys. **67**, 314–329 (2020)
9. Aly, E.H., Ebaid, A.: MHD Marangoni boundary layer problem for hybrid nanofluids with thermal radiation. Int. J Numer. Method H. (2020). https://doi.org/10.1108/HFF-05-2020-0245
10. Hayat, T., Nadeem, S., Khan, A.U.: Numerical analysis of $Ag - CuO$/water rotating hybrid nanofluid with heat generation and absorption. Can. J. Phys. (2018). https://doi.org/10.1139/cjp-2018-0011
11. Eshgarf, H., Kalbasi, R., Maleki, A., Shadloo, M.S., karimipour, A.: A review on the properties, preparation, models and stability of hybrid nanofluids to optimize energy consumption. J. Therm. Anal. Calorim. (2020). https://doi.org/10.1007/s10973-020-09998-w
12. Abdelsalam, S.I., Velasco-Hernández, J.X., Zaher, A.Z.: Electro-magnetically modulated self-propulsion of swimming sperms via cervical canal. Biomech. Model. Mechanobiol. **20**, 861–878 (2021)
13. Raza, R., Mabood, F., Naz, R., Abdelsalam, S.I.: Thermal transport of radiative Williamson fluid over stretchable curved surface. Therm. Sci. Eng. Prog. **23**, 100887 (2021)
14. Adewale, F.J., Lucky, A.P., Oluwabunmi, A.P., Boluwaji, E.F.: Selecting the most appropriate model for rheological characterization of synthetic based drilling mud. Int. J. Appl. Eng. Res. **12**(18), 7614 (2017). (**ISSN 0973-4562**)
15. Aman, S., Zokri, S.M., Ismail, Z., Salleh, M.Z., Khan, I.: Casson model of MHD flow of SA-based hybrid nanofluid using caputo time-fractional models. Defect Diffus. Forum. **390**, 83–90 (2019)
16. Jamshed, W., Aziz, A.: Cattaneo-Christov based study of $TiO_2 - CuO/EG$ Casson hybrid nanofluid flow over a stretching surface with entropy generation. Appl. Nanosci. **8**, 685–698 (2018)
17. Muhammad, T., Lu, D., Mahanthesh, B., Eid, M.R., Ramzan, M., Dar, A.: Significance of Darcy-Forchheimer porous medium in nanofluid through carbon nanotubes. Commun. Theor. Phys. **70**(3), 361–366 (2018)
18. Eid, M.R., Mabood, F.: Two-phase permeable non-Newtonian cross-nanomaterial flow with Arrhenius energy and entropy generation: Darcy-Forchheimer model. Phys. Scr. **95**(10), 105209 (2020)
19. Vishnu Ganesh, N., Abdul Hakeem, A.K., Ganga, B.: Darcy-Forchheimer flow of hydromagnetic nanofluid over a stretching/shrinking sheet in a thermally stratified porous medium with second order slip, viscous and Ohmic dissipations effects. Ain Shams Eng. J. **9**(4), 939–951 (2018)

20. Eldesoky, I.M., Abdelsalam, S.I., El-Askary, W.A., El-Refaey, A.M., Ahmed, M.M.: Joint Effect of Magnetic Field and Heat Transfer on Particulate Fluid Suspension in a Catheterized Wavy Tube. Bio-NanoScience. **9**, 723–739 (2019)
21. Rasool, G., Chamkha, A.J., Muhammad, T., Shafiq, A., Khan, I.: Darcy-Forchheimer relation in Casson type MHD nanofluid flow over non-linear stretching surface. Propuls. Power Res. **9**(2), 159–168 (2020)
22. Ferdows, M., Nabwey, H.A., Rashad, A.M., Uddin, M.J.: Alzahrani, Faris: Boundary layer flow of a nanofluid past a horizontal flat plate in a Darcy porous medium: A Lie group approach. Proc Inst Mech Eng C J Mech Eng Sci **234**(8), 1545–1553 (2020)
23. Gul, T., Rahman, J.U., Bilal, M., Saeed, A., Alghamdi, W., Mukhtar, S., Alrabaiah, H., Bonyah, E.: Viscous dissipated hybrid nanoliquid flow with Darcy-Forchheimer and forced convection over a moving thin needle. AIP Adv. **10**, 105308 (2020)
24. Eid, M.R., Makinde, O.D.: Solar radiation effect on a magneto nanofluid flow in a porous medium with chemically reactive species. Int. J. Chem. React. Eng. **16**(9), 20170212 (2018)
25. Tlau, L., Ontela, S.: Mixed convection nanofluid flow in a non-Darcy porous medium with variable permeability: entropy generation analysis. Indian J. Phys. (2020). https://doi.org/10.1007/s12648-020-01856-7
26. Zaib, A., Haq, R.U., Sheikholeslami, M., Chamkha, A.J., Rashidi, M.M.: Impact of non-darcy medium on mixed convective flow towards a plate containing micropolar water-based TiO_2 nanomaterial with entropy generation. J. Porous Media. **23**(1), 11–26 (2020)
27. Manh, T.D., Tlili, I., Shafee, A., Nguyen-Thoi, T., Hamouda, H.: Modeling of hybrid nanofluid behavior within a permeable media involving buoyancy effect. Phys. A **554**, 123940 (2020)
28. Mabood, F., Ibrahim, S.M., Kumar, P.V., Lorenzini, G.: Effects of slip and radiation on convective MHD Casson nanofluid flow over a stretching sheet influenced by variable viscosity. J. Engin. Thermophys. **29**, 303–315 (2020)
29. Abdul Hakeem, A.K., Vishnu Ganesh, N., Ganga, B.: Heat transfer of non-Darcy MHD ow of a nano fluid over a stretching/shrinking surface in a thermally stratified medium with second order slip model. Sci. Iran. F **22**(6), 2766–2784 (2015)
30. Anuar, N.S., Bachok, N., Arifin, N.M., Rosali, H., Pop, I.: Stagnation-point flow and heat transfer over an exponentially stretching/shrinking sheet in hybrid nanofluid with slip velocity effect: stability analysis. J. Phys.: Conf. Ser. **1366**, 012002 (2019)
31. Elmaboud, Y.A., Mekheimer, K.S., Abdelsalam, S.I.: A study of nonlinear variable viscosity in finite-length tube with peristalsis. Appl Bionics Biomech. **11**, 197–206 (2014)
32. Sreenivasulu, P., Poornima, T., Malleswari, B., Bhaskar Reddy, N., Souayeh, B.: Viscous dissipation impact on electrical resistance heating distributed Carreau nanoliquid along stretching sheet with zero mass flux. Eur. Phys. J. Plus. **135**(9), 1–25 (2020)
33. Ahmad, S., Nadeem, S.: Cattaneo-Christov-based study of $SWCNT\text{-}MWCNT/EG$ Casson hybrid nanofluid flow past a lubricated surface with entropy generation. Appl. Nanosci. **10**, 5449–5458 (2020). https://doi.org/10.1007/s13204-020-01367-1
34. Kala, K.S.: Analysis of non-Darcy MHD flow of a Casson fluid over a non-linearly stretching sheet with partial slip in a porous medium. Asian J. Advanced Research Reports.AJARR.47539 **3**(3), 1–15 (2019)
35. Khan, U., Zaib, A., Khan, I., Baleanu, D., Nisar, K.S.: Enhanced heat transfer in moderately ionized liquid due to hybrid MoS_2/SiO_2 nanofluids exposed by nonlinear radiation: stability analysis. Curr. Comput.-Aided Drug Des. **10**(2), 142 (2020)
36. Qawasmeh, B.R., Alrbai, M., Al-Dahidi, S.: Forced convection heat transfer of Casson liquid in non-Darcy porous media. Adv. Mech. Eng. **11**(1), 1–10 (2019)
37. Chamkha, A.J., Mujtaba, M., Quadri, A., Issa, C.: Thermal radiation effects on MHD forced convection flow adjacent to a non-isothermal wedge in the presence of a heat source or sink. Heat Mass Transf. **39**, 305–312 (2003)
38. Lin, H.T., Lin, L.K.: Similarity solutions for laminar forced convection heat transfer from wedges to fluids of any Prandtl number. Int. J. Heat Mass Transf. **30**, 1111–1118 (1987)